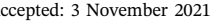
RESEARCH ARTICLE





Check for updates

Polymer coating with gradient-dispersed dielectric nanoparticles for enhanced daytime radiative cooling

| Yidan An¹ | Yunkun Xu¹ | Jian-Guo Dai² | Dangyuan Lei¹ o

Correspondence

Dangyuan Lei, Department of Materials Science and Engineering, City University of Hong Kong, 83 Tat Chee Avenue, Kowloon, Hong Kong, 999077, China. Email: dangylei@cityu.edu.hk

Funding information

City University of Hong Kong, Grant/ Award Number: 9610434

Abstract

Polymeric coatings with randomly distributed dielectric nanoparticles have attracted intensive attention in the passive daytime radiative cooling application. Here, we propose a modified Monte-Carlo method for investigating the spectral response and cooling performance of polymer coating with gradientdispersed nanoparticles. Using this method, we carry out a quantitative analysis on the solar reflectance, infrared emittance and cooling power of four categories of gradient structures. It is shown that the gradient profile of particle distribution at the near-surface region has a significant influence on the overall performance of the coatings. Compared to a randomly distributed structure, the downward size-gradient structure exhibits superiority in both solar reflectance and cooling power. The presented gradient design, also applicable to porous structures, provides an effective and universal strategy for significantly improving the cooling performance of radiative cooling coatings.

KEYWORDS

dielectric nanoparticles, gradient structures, Mie scattering, Monte-Carlo simulation, polymeric coating, radiative cooling

INTRODUCTION 1

Passive daytime radiative cooling as a promising energy conservation strategy has shown great potential for saving the building energy, mitigating the urban heat island effect and combatting global warming.^{1,2} Compared to conventional active refrigeration technologies, it takes advantages of the passive nature of thermal radiation and the transparent atmospheric window (8–13 µm) to dissipate heat from a terrestrial object (~300 K) to the cold universe (~3 K). Anti-intuitive sub-ambient radiative cooling without any energy consumption and green-house gas emission can be achieved even under direct sunlight.^{3,4} To maximize the cooling effect, the radiative cooler should be entitled with high emissivity within the atmospheric window and high solar reflectance simultaneously. Recently, photonic structures, 3,5-7 metamaterials, 8-11 particle dispersed polymeric coatings, 12-15 and porous structures¹⁶⁻²¹ have been investigated to simultaneously achieve high solar reflectance as well as high infrared radiation. Among these methods, polymeric coatings have shown the best potential for real-world large-scale applications for its low cost, ease in production and excellent long-term durability.²²

Generally, polymeric coatings consist of a polymer matrix and randomly distributed micro/nano dielectric particles as fillers. The high thermal radiation originates mainly from the intrinsic vibrational modes of functional groups/bonds of the polymer matrix and partially from the phonon resonances of filled particles, 9,23 while the

1 of 8

This is an open access article under the terms of the Creative Commons Attribution License, which permits use, distribution and reproduction in any medium, provided the original work is properly cited.

© 2022 The Authors. EcoMat published by The Hong Kong Polytechnic University and John Wiley & Sons Australia, Ltd.

¹Department of Materials Science and Engineering, City University of Hong Kong, Hong Kong, China

²Department of Civil and Environmental Engineering, The Hong Kong Polytechnic University, Hong Kong, China

25673173, 2022. 2, Dowlonded from https://onlinelibrary.wiley.com/doi/10.1002/com2.12169 by City University Of Hong Kong, Wiley Online Library on [16/12/2024]. See the Terms and Conditions (https://onlinelibrary.wiley. and-conditions) on Wiley Online Library for rules of use; OA articles are governed by the applicable Creative Commons Licensa

high solar reflectance of the coatings benefits from the multiple interfacial Mie scattering between the polymer matrix and the filled particles.²⁴ Therefore, materials with a high refractive index and large band gap are preferred for use as fillers to enhance Mie scattering and thus the overall solar reflectance. Various numerical and experimental studies have explored different strategies for optimizing such scattering effect based on changing key parameters such as particle size, volume fraction and coating thickness, for which different fillers (e.g., TiO2, BaSO4, Al₂O₃, CaCO₃) have been utilized to scatter the incident sunlight in a random-dispersed and multiple-sized manner. 6,12-14,25 However, when mixing the nanoparticles and liquid polymer solution, sedimentation always occurs due to the gravity effect and results in the size and density gradients.²⁶⁻²⁸ In other words, a heterogeneous distribution may be formed instead of an ideal homogeneous one during the formation of the polymeric nanocomposite coating. In general, the gradient distribution caused by sedimentation was utilized to separate different species with different mass and sizes.²⁹ Inspired by natural/ biological materials, artificial control of gradient structure has been also studied to facilitate functional graded materials with tunable performance, e.g., reinforcement of mechanical properties, thermal properties, electromagnetic properties and optical properties. 30-35

In this study, we numerically investigate the optical properties of a polymeric coating from ultra-violet to mid-far infrared regions, as well as its cooling potential, using both density- and size-gradient structures. An effective multilayer Monte–Carlo method is established to solve the radiative transfer equation for the gradient structures, of which the solar reflectance, infrared emittance and net cooling power are investigated. We have observed an obvious impact of gradient distribution on the cooling performance of the coating and the downward size-gradient structure is superior to the randomly distributed one.

2 | MATERIALS AND METHODS

2.1 | Materials and optical constants

Many kinds of polymers, including polydimethylsiloxane (PDMS), polymethyl methacrylate (PMMA), polyvinylidene fluoride (PVDF), polymethyl pentene (TPX), etc., have been used as the polymer matrix that makes the radiative cooler feature low solar absorption and strong thermal emissivity ascribing to the functional groups such as C—O, C—F, C—H, and O—H. In this study, PDMS is chosen as the polymer matrix due to its lower refractive index (~1.4 within the solar band) and good infrared

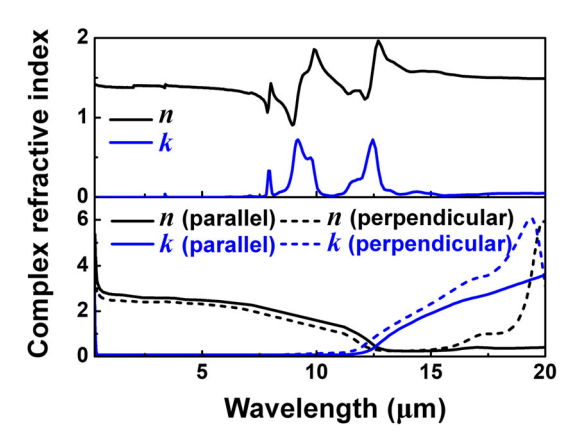


FIGURE 1 Real part (dark) and imaginary part (blue) of complex refractive indices of PDMS (top panel, Adapted with permission from: Copyright 2020, Elsevier³⁷ and Copyright 2020, Optical Society of America³⁸) and TiO_2 (bottom panel, solid line for parallel polarization and dashed line for perpendicular polarization)³⁹

emissivity within the atmospheric window.³⁶ The refractive index and extinction coefficient are shown in the top panel of Figure 1 according to the measurement by Zhang et al.^{37,38}

Nano-sized dielectric fillers can significantly boost the solar reflectivity through Mie scattering; therefore, an appropriate filler should be selected with consideration of its complex refractive index. The real part, refractive index n, should be high enough than the polymer matrix to achieve an excellent scattering efficiency according to Mie theory, while the imaginary part, extinction coefficient k, needs to be as low as possible to diminish the parasitic absorption under illumination. Therefore, dielectric materials with large bandgap (over 6 eV), such as BaSO₄, Al₂O₃, and CaCO₃, are preferred in order to reduce solar absorption. Nevertheless, the refractive indices of these dielectric materials are around 1.6-1.7 over the solar spectrum, which are slightly higher than most polymer matrices. The rutile TiO₂, however, retains the refractive index over 2.4 within the solar spectrum and are widely used as a commercial coating component, as shown in the bottom panel of Figure 1.39 Hence, we chose TiO₂ as the filler to take full advantage of Mie scattering. Though TiO2 bears intrinsic UV absorption owing to a bandgap of ~3 eV, it can be minimized by a recently proposed Purcell-effect-enhancedfluorescence method, in which the fluorescent materials compete with TiO2 in UV absorption that can be converted and re-emitted as visible light.²²

2.2 | Theories and methods

To investigate the spectral solar reflectivity and infrared emissivity, a statistical Monte-Carlo method, in which a mass number of light paths are traced, rather than finite element method is applied to reduce the computational efforts. The required scattering and absorption properties of both medium and particles will be obtained by Mie theory, and then coupled with the radiative transfer equations (RTE) which will be solved in the Monte–Carlo model.

2.2.1 | Mie theory

For each single particle in the medium, the scattering efficiency, extinction efficiency and asymmetry parameter can be calculated by solving Maxwell equations^{40,41}:

$$Q_{\text{sca}} = \frac{2}{x^2} \sum_{n=1}^{\infty} (2n+1) (|a_n|^2 + |b_n|^2)$$
 (1)

$$Q_{\text{ext}} = \frac{2}{x^2} \sum_{n=1}^{\infty} (2n+1) \text{Re}\{a_n + b_n\}$$
 (2)

$$g = \frac{4}{Q_{\text{sca}} x^2} \left[\sum_{n=1}^{\infty} \frac{n(n+2)}{n+1} Re \left\{ a_n a_{n+1}^* + b_n b_{n+1}^* \right\} + \sum_{n=1}^{\infty} \frac{2n+1}{n(n+1)} Re \left\{ a_n b_n^* \right\} \right]$$
(3)

where x is the size parameter defined by the particle size, wavelength and refractive index of polymer matrix, a_n , b_n , a_n^* , and b_n^* are the Mie coefficients and their conjugates. In the Monte–Carlo calculation for a nanoparticle-polymer composite, the uniform distribution leads to a layer of effective medium. The effective properties of the coating can be directly obtained by accumulating all the parameters of fillers. However, the gradient distribution of particles creates a continuous but non-homogenous phase that cannot be regarded as a single layer effective medium. Here, we treat the gradient structure as many thinner sublayers, and every sublayer could be considered as homogeneous. Then the effective scattering and absorption properties of the ith sublayer become:

$$\sigma_{i,\lambda} = \sum \frac{3f_{i,j}Q_{\text{sca},j}}{4r_j} \tag{4}$$

$$\kappa_{i,\lambda} = \sum \frac{3f_{i,j}Q_{\text{abs},j}}{4r_i} + \frac{4\pi k_{\text{mat}}}{\lambda}$$
 (5)

where the subscript j represents the jth kind of particle, $f_{i,j}$ is the corresponding volume fraction in ith sublayer, r_i is corresponding radius, k_{mat} is the extinction

coefficient of polymer matrix. Since TiO₂ particles shows different complex refractive indices for parallel and perpendicular polarization, here the same amount of TiO₂ particles is assumed for both polarizations in the

2.2.2 | Modified Monte-Carlo method

coating.12

The spectral reflectance and emittance of the coating can be estimated by solving the quasi-steady form of radiative transfer equation⁴¹:

$$\frac{\mathrm{d}I_{\lambda}}{\mathrm{d}s} = \kappa_{\lambda}I_{b,\lambda} - (\kappa_{\lambda} + \sigma_{\lambda})I_{\lambda} + \frac{\sigma_{\lambda}}{4\pi} \int I_{\lambda}(\hat{\mathbf{s}}_{i})\Phi_{\lambda}(\hat{\mathbf{s}}_{i},\hat{\mathbf{s}})\mathrm{d}\Omega' \qquad (6)$$

where I_{λ} and $I_{b,\lambda}$ are the spectral radiative intensities of the coating and a blackbody, s denotes the geometric path of radiative transfer, $\Phi_{\lambda}(\hat{s}_i, \hat{s})$ is the scattering phase function describing the scattering probability from direction \hat{s}_i to direction \hat{s} of the incoming heat flux at solid angle of $d\Omega'$, κ_{λ} and σ_{λ} are the effective properties obtained by Equations (4) and (5).

As mentioned above, Monte–Carlo method was implemented to solve RTE in coatings with random particle distribution and achieved good feasibility for photon transport estimation. However, to evaluate the optical properties of gradient structures, a new calculation method should be developed to quantitatively estimate the spectral responses of the coating considering such inhomogeneity. In addition to the multi-sublayer assumption, the interfacial effect is neglected when the light propagates from one sublayer to another due to their same matrix. The flowchart of modified Monte–Carlo method used for gradient structures is shown in Figure 2. Random numbers (RN) are used in the model to statistically trace the light path. Effective properties of sublayers and scattering features of particles are marked using the layer flag *i* and particle type flag *j*, respectively.

2.2.3 | Radiative cooling performance

Two key parameters, net cooling power at ambient temperature $P_{\rm net}$ and sub-ambient temperature difference ΔT at the thermodynamic equilibrium state, were usually deployed to evaluate the cooling performance of the radiative cooler. While for a typical application (e.g., on building envelope), the coatings are always at near or above the ambient temperature due to thermal interaction with surrounding urban environment and indoor heat generation. Hence, here we calculate the net cooling power only for estimating the cooling performance of the gradient structured coating.

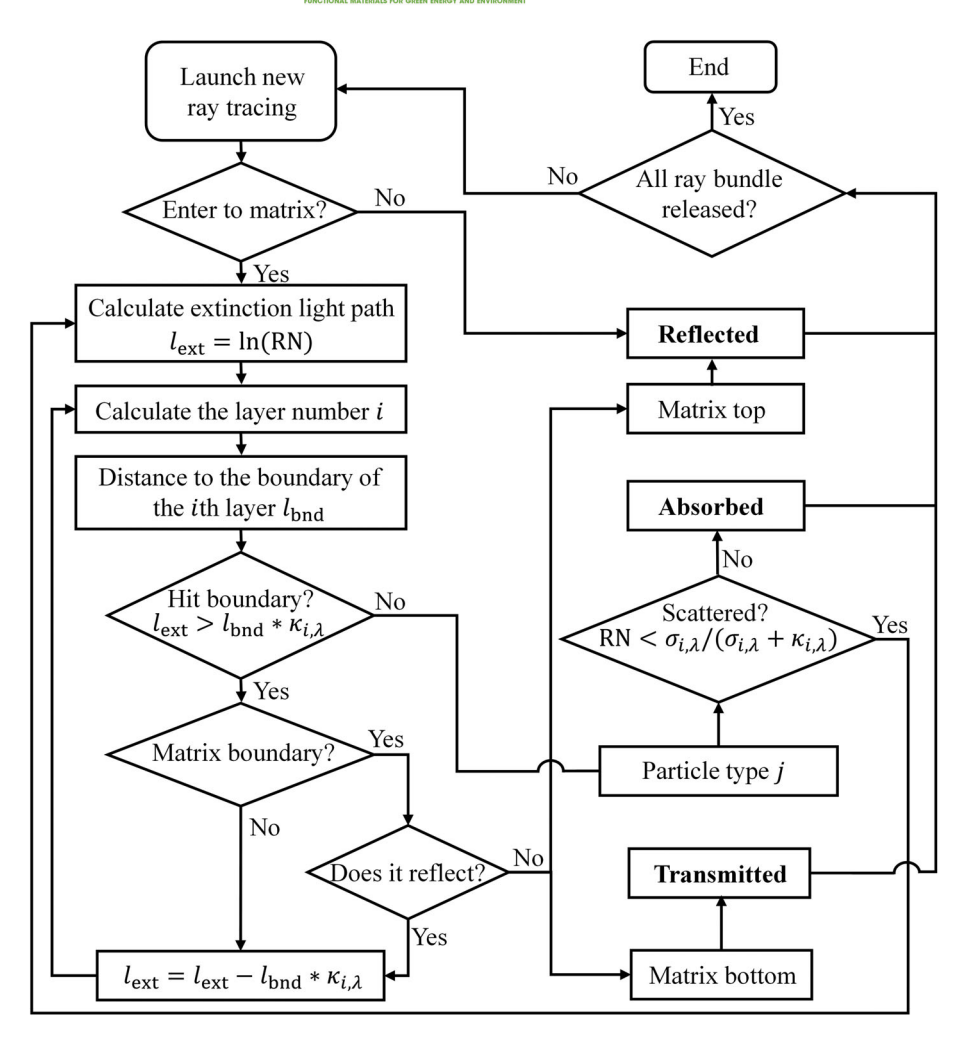


FIGURE 2 Flowchart of the modified Monte–Carlo method for analyzing the spectral response of gradient structures with multi-sublayer and multi-sized particles

Considering all the thermal exchange processes, the net cooling power P_{net} of a radiative cooler at temperature T can be expressed as³:

$$P_{\text{net}}(T) = P_{\text{rad}}(T) - P_{\text{atm}}(T_{\text{amb}}) - P_{\text{sol}} - P_{\text{non-rad}}$$
 (7)

where $P_{\rm rad}$ is the radiated power by the cooler, $P_{\rm atm}$, $P_{\rm sol}$, and $P_{\rm non-rad}$ are the absorbed power of atmospheric radiation, solar irradiation and non-radiative (conductive and convective) thermal energy, respectively, $T_{\rm amb}$ (= 300 K) is the typical temperature of an ambient environment. Each thermal exchange process can be described as:

$$P_{\rm rad}(T) = 2\pi \int_{0}^{\infty} \int_{0}^{\pi/2} \varepsilon(\lambda, \theta, T) I_{\rm BB}(T, \lambda) \cos\theta \sin\theta d\theta d\lambda \quad (8)$$

$$\begin{split} P_{\rm atm}(T_{\rm amb}) &= \\ 2\pi \int_{0}^{\infty} \int_{0}^{\pi/2} \varepsilon(\lambda, \theta, T) \varepsilon_{\rm atm}(\lambda, \theta) I_{\rm BB}(T_{\rm atm}, \lambda) {\rm cos} \theta {\rm sin} \theta {\rm d} \theta {\rm d} \lambda \end{split} \tag{9}$$

$$P_{\text{sol}} = \cos\theta_{\text{sun}} \int_{0}^{\infty} \varepsilon(\lambda, \theta, T) I_{\text{solar}}(\lambda) d\lambda$$
 (10)

$$P_{\text{non-rad}} = h_{\text{eff}}(T_{\text{amb}} - T) \tag{11}$$

where $\varepsilon(\lambda,\theta,T)$ is the angular spectral emissivity of the cooler, $I_{\rm BB}(T,\lambda)$ is the spectral radiance of blackbody at temperature T, $\varepsilon_{\rm atm}(\lambda,\theta)$ is the angular dependent emissivity of the atmosphere that is related to the atmospheric transparency in the zenith direction. 42 $\theta_{\rm sun}$ is the angle between the sun and zenith direction. $h_{\rm eff}$ is the effective coefficient of non-radiative heat transfer. Here, the temperature of the cooler is assumed to be the same as the ambient, thus the non-radiative contribution will be neglected, that is, $P_{\rm non-rad}=0$.

3 | RESULTS AND DISCUSSIONS

3.1 | Validation of modified Monte-Carlo method

First, for validating the effeteness of our developed Monte-Carlo method, the optical properties of random particle distribution coating are calculated under both methods (i.e., the traditional one and the modified one) for comparison, where the coating is assumed to consist of 100 µm thick PDMS and randomly distributed TiO₂ nanoparticles with a volume fraction of f = 0.05 and uniform radius of r = 200 nm. The obtained reflectivity at solar range and emissivity at infrared band from both methods matched perfectly each other, as shown in Figure 3, which proves the feasibility of the multisublayer assumption and neglecting the interfacial effect. Here, the 100 µm thick coating is divided into 5, 10, and 20 sublayers with the sublayer thickness of 20, 10, and 5 μm for the modified Monte–Carlo method, respectively.

Density-gradient and size-gradient structures

In practice, the sedimentation effect may lead to the formation of four gradient distributions of particles, incorporating two types of gradients (i.e., density-gradient and size-gradient) and two directions of gradients (i.e., downward and upward). As shown in Figure 4, downward gradient manifests that the size or volume fraction gradually increases from the top boundary to the bottom boundary of the coating while the upward gradient features the opposite trend. To explore the optical properties and cooling performance of the density-gradient coating, the overall solar reflectance and infrared emittance are calculated using the modified Monte-Carlo method and are shown in Figure 5A,B, where the 300 µm thick PDMS coating is filled with TiO_2 nanoparticles at a uniform radius of r = 200nm. By increasing the volume fractions at the boundaries (f_{top}) , at the top boundary and f_{bot} , at the bottom boundary) from 0.01 to 0.3, we can clearly see that both the reflectance and emittance are significantly boosted. Therefore, the best cooling performance can be obtained at the highest volume fraction (i.e., $f_{top} = f_{bot} = 0.3$), as shown in Figure 5C. Moreover, it should be noticed that the upward gradient coating outperforms the downward gradient one in the solar reflectance since a higher volume fraction of TiO₂ at the top boundary can scatter the sunlight more efficiently.

Further, the optical and cooling characteristics of size-gradient coating is investigated in Figure 5D-F, where the particle radii at the boundaries (r_{top} at top boundary and r_{bot} at bottom boundary) vary from 100 to 1000 nm. It can be observed that the downward sizegradient coating exhibits a superior solar reflectance compared to its upward size-gradient counterpart. Since the scattering efficiency of TiO₂ nanoparticles approaches the maximum at the radius around 100-200 nm and gradually falls down at larger sizes, 25 downward size-gradient coating that has smaller particles at the top always

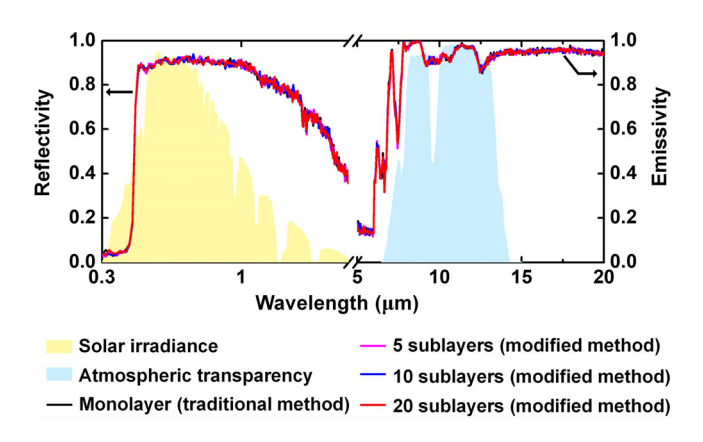


FIGURE 3 Reflectivity (left y axis) and emissivity (right y axis) of 100 µm thick PDMS-TiO₂ coating calculated by both traditional Monte-Carlo method (black line) and the modified one (magenta, blue and red lines for 5, 10, and 20 sublayers, respectively)

scatters the sunlight more efficiently than the upward size-gradient coating except for the case denoted by a red triangle in Figure 5D, in which the particles at the top $(r_{top} = 100 \text{ nm})$ has a slightly lower scattering efficiency than the bottom ($r_{top} = 200$ nm). Finally, the spectral properties and cooling performance of the coating with random particle distribution are calculated in Figure 5G-I through the traditional Monte-Carlo method for comparison. It can be seen that the solar reflectance manifests a similar reduction with increasing the size of particles. However, we can see obvious differences between the random distribution and upward/downward size-gradient structures. For example, comparing to the downward sizegradient structure, the randomly distributed structure exhibits a larger reduction of solar reflectance and a marginal improvement of infrared emissivity when the size distribution is broadened. An opposite trend is observed between the randomly distributed and upward size-gradient structures.

Detailed comparisons of the spectral properties and cooling performance are demonstrated in Figure 6. It can be observed that at a broad size distribution (r = 100 - 1000nm), the downward size-gradient structure leads to a superior solar reflectivity and considerable infrared emissivity as shown in Figure 6A. The randomly distributed structure exhibits a better infrared emissivity at the wavelength below 6 µm, while the downward size-gradient structure leads to a higher infrared emissivity at the range of 6–9 μm and 13–20 μm. Thus, although the downward size-gradient structure does not perform the best infrared emissivity, its superior solar reflectivity enables an extra cooling power up to ~36 W/m2 than the randomly distributed structure, as shown in Figure 6B. On the contrary, the upward gradient distribution shows poorer performance for both solar reflectivity and

25673173, 2022, 2, Downlo

library.wiley.com/doi/10.1002/com2.12169 by City University Of Hong Kong, Wiley Online Library on [16/12/2024], See the Terms

conditions) on Wiley Online Library for rules of use; OA articles are governed by the applicable Creative Commons

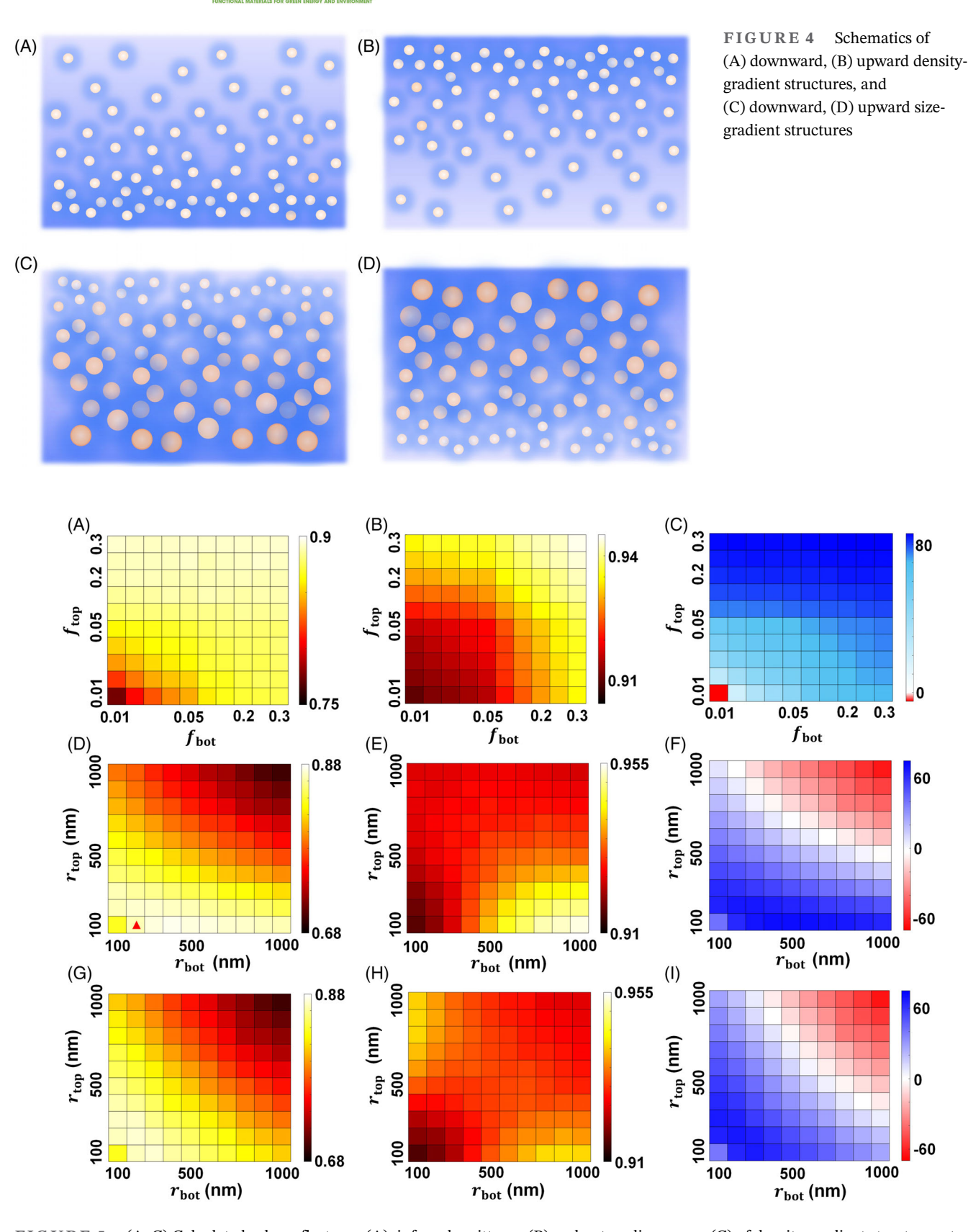


FIGURE 5 (A–C) Calculated solar reflectance (A), infrared emittance (B) and net cooling power (C) of density-gradient structures at ambient temperature. The size of TiO_2 is fixed as r=200 nm. (D–F) Solar reflectance (D), infrared emittance (E) and net cooling power (F) of size-gradient structures at ambient temperature. The volume fraction is fixed as f=0.05. (G–I) Solar reflectance (G), infrared emittance (H) and net cooling power (I) of randomly distributed structures at ambient temperature. The volume fraction is also fixed as f=0.05. The thickness of all the coatings is $300\,\mu m$

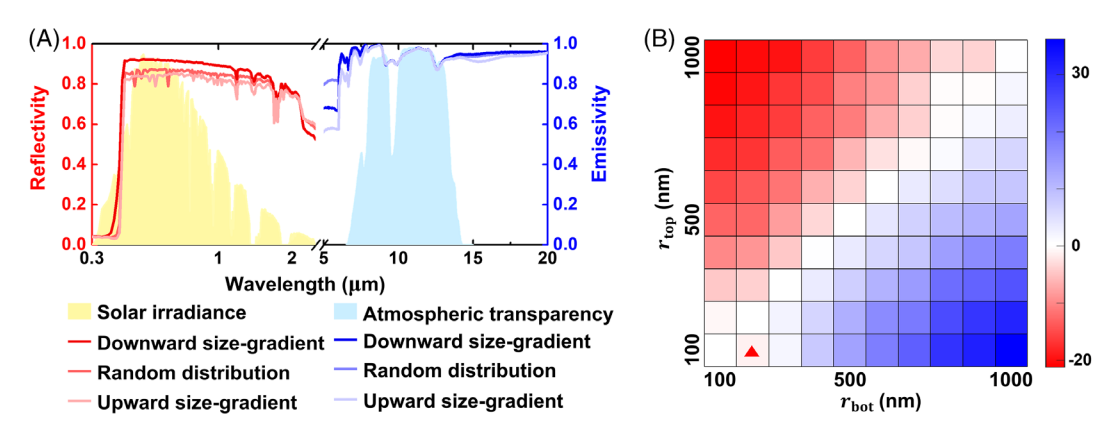


FIGURE 6 (A) Comparison of solar reflectivity (red) and infrared emissivity (blue) among a randomly distributed structure, a downward size-gradient structure and an upward size-gradient structure with the size distribution from 100 to 1000 nm. (B) Difference of net cooling power between size-gradient structures and randomly distributed structures at ambient temperature. The volume fraction of TiO_2 particles in PDMS and the coating thickness are f=0.05 and $300 \, \mu m$, respectively. The red triangle denotes the exceptional superiority of downward size-gradient structures

infrared emissivity, and thus the cooling power. It should be noticed that there is an exception for cooling power difference in Figure 6B, which corresponds to the reflectance exception in Figure 5D. Based on our calculation results, the downward size gradient, which could be naturally formed during the production of an actual coating, may enable further enhancement of the cooling performance than the random size distribution. Such structure can also be intentionally utilized to configure the coating for better cooling performance in future.

4 | CONCLUSION

Considering the sedimentation effect during curing of polymer coating, we have explored the spectral properties and cooling potentials for gradient structures under two types and two directions of gradients. Traditional Monte-Carlo method is modified through multiple sublayers simplification while ignoring the interfacial effect. A significant impact of gradient distribution on the coating performance is observed. The upward density-gradient and downward size-gradient perform better in all four studied gradient structures because the light interacts with particles at the top of the coating first. Compared to the randomly distributed structure, the downward size-gradient structure leads to an improvement of the cooling power up to $\sim 36 \text{ W/m}^2$ at a broad size distribution, while upward size-gradient structure behaves the opposite. Therefore, though the sedimentation effect was not considered in previous studies, the construction procedure may produce the size gradient to an extent, resulting in a better cooling performance than the prediction based on the random distribution assumption. The findings arisen from the present theoretical study has shed light on how to optimize the performance of a radiative cooling coating through introducing gradient-distributed nanoparticles into the polymer matrix.

ACKNOWLEDGMENTS

This work was funded by The City University of Hong Kong (Project No. 9610434).

CONFLICT OF INTEREST

The authors declare no conflict of interest.

ORCID

Dangyuan Lei https://orcid.org/0000-0002-8963-0193

REFERENCES

- 1. Yin X, Yang R, Tan G, Fan S. Terrestrial radiative cooling: using the cold universe as a renewable and sustainable energy source. *Science*. 2020;370(6518):786-791.
- Center BP. Annual Energy Outlook 2020. Washington, DC: Energy Information Administration; 2020.
- Raman AP, Abou Anoma M, Zhu L, Rephaeli E, Fan S. Passive radiative cooling below ambient air temperature under direct sunlight. *Nature*. 2014;515(7528):540-544.
- 4. Chen Z, Zhu L, Raman A, Fan S. Radiative cooling to deep sub-freezing temperatures through a 24-h day–night cycle. *Nat Commun*. 2016;7(1):1-5.
- 5. Li W, Shi Y, Chen Z, Fan S. Photonic thermal management of coloured objects. *Nat Commun*. 2018;9(1):1-8.
- Zhang H, Ly KC, Liu X, et al. Biologically inspired flexible photonic films for efficient passive radiative cooling. *PNAS*. 2020; 117(26):14657-14666.
- 7. Sheng C, An Y, Du J, Li X. Colored radiative cooler under optical Tamm resonance. *ACS Photon*. 2019;6(10):2545-2552.
- 8. Zou C, Ren G, Hossain MM, et al. Metal-loaded dielectric resonator metasurfaces for radiative cooling. *Adv Opt Mater.* 2017; 5(20):1700460.

- 9. Zhai Y, Ma Y, David SN, et al. Scalable-manufactured randomized glass-polymer hybrid metamaterial for daytime radiative cooling. *Science*. 2017;355(6329):1062-1066.
- 10. Jeong S, Tso CY, Wong YM, Chao CY, Huang B. Daytime passive radiative cooling by ultra emissive bio-inspired polymeric surface. *Sol Energy Mater sol Cells*. 2020;206:110296.
- Lu Y, Chen Z, Ai L, et al. A universal route to realize radiative cooling and light management in photovoltaic modules. Sol RRL. 2017;1(10):1700084.
- Huang Z, Ruan X. Nanoparticle embedded double-layer coating for daytime radiative cooling. *Int J Heat Mass Transfer*. 2017;104:890-896.
- 13. Li X, Peoples J, Huang Z, Zhao Z, Qiu J, Ruan X. Full daytime sub-ambient radiative cooling in commercial-like paints with high figure of merit. *Cell Rep Phys Sci.* 2020;1(10):100221.
- 14. Li X, Peoples J, Yao P, Ruan X. Ultrawhite BaSO4 paints and films for remarkable daytime subambient Radiative cooling. *ACS Appl Mater Interfaces*. 2021;13(18):21733-21739.
- Ma H, Wang L, Dou S, et al. Flexible daytime Radiative cooling enhanced by enabling three-phase composites with scattering interfaces between silica microspheres and hierarchical porous coatings. ACS Appl Mater Interfaces. 2021;13(16):19282-19290.
- Mandal J, Fu Y, Overvig AC, et al. Hierarchically porous polymer coatings for highly efficient passive daytime radiative cooling. *Science*. 2018;362(6412):315-319.
- Fu Y, Yang J, Su Y, Du W, Ma Y. Daytime passive radiative cooler using porous alumina. Sol Energy Mater Sol Cells. 2019;191:50-54.
- 18. Kang MH, Lee GJ, Lee JH, et al. Outdoor-useable, wireless/battery-free patch-type tissue oximeter with radiative cooling. *Adv Sci.* 2021;2004885(10):2004885.
- 19. Li T, Zhai Y, He S, et al. A radiative cooling structural material. *Science*. 2019;364(6442):760-763.
- Wang T, Wu Y, Shi L, Hu X, Chen M, Wu L. A structural polymer for highly efficient all-day passive radiative cooling. *Nat Commun.* 2021;12(1):1-11.
- 21. Li D, Liu X, Li W, et al. Scalable and hierarchically designed polymer film as a selective thermal emitter for high-performance all-day radiative cooling. *Nat Nanotechnol.* 2021;16(2):153-158.
- 22. Xue X, Qiu M, Li Y, et al. Creating an eco-friendly building coating with smart subambient Radiative cooling. *Adv Mater*. 2020;32(42):1906751.
- Mandal J, Yang Y, Yu N, Raman AP. Paints as a scalable and effective radiative cooling technology for buildings. *Joule*. 2020; 4(7):1350-1356.
- Yalçın RA, Blandre E, Joulain K, Jrm D. Colored Radiative cooling coatings with nanoparticles. ACS Photon. 2020;7(5): 1312-1322.
- 25. Peoples J, Li X, Lv Y, Qiu J, Huang Z, Ruan X. A strategy of hierarchical particle sizes in nanoparticle composite for enhancing solar reflection. *Int J Heat Mass Transfer*. 2019;131: 487-494.
- 26. Tong P, Ye X, Ackerson BJ, Fetters L. Sedimentation of colloidal particles through a polymer solution. *Phys Rev Lett.* 1997; 79(12):2363-2366.

- Langevin D, Rondelez F. Sedimentation of large colloidal particles through semidilute polymer solutions. *Polymer*. 1978;19(8): 875-882
- 28. Liu YJ, Joseph DD. Sedimentation of particles in polymer solutions. *J Fluid Mech.* 1993;255(1):565-595.
- Laurent TC, Pietruszkiewicz A. The effect of hyaluronic acid on the sedimentation rate of other substances. *Biochim Biophys Acta*. 1961;49(2):258-264.
- 30. Wu X, Jiang P, Chen L, Yuan F, Zhu YT. Extraordinary strain hardening by gradient structure. *PNAS*. 2014;111(20):7197-7201.
- 31. Liu Z, Meyers MA, Zhang Z, Ritchie RO. Functional gradients and heterogeneities in biological materials: design principles, functions, and bioinspired applications. *Prog Mater Sci.* 2017; 88:467-498.
- Mueller E, Drašar Č, Schilz J, Kaysser W. Functionally graded materials for sensor and energy applications. *Mater Sci Eng A*. 2003;362(1–2):17-39.
- 33. Smith DR, Mock JJ, Starr A, Schurig D. Gradient index metamaterials. *Phys Rev E*. 2005;71(3):036609.
- 34. Chen M, Zhu Y, Pan Y, Kou H, Xu H, Guo J. Gradient multi-layer structural design of CNTs/SiO2 composites for improving microwave absorbing properties. *Mater des.* 2011;32(5):3013-3016.
- Cherradi N, Kawasaki A, Gasik M. Worldwide trends in functional gradient materials research and development. *Compos Eng.* 1994;4(8):883-894.
- Kou J-l, Jurado Z, Chen Z, Fan S, Minnich AJ. Daytime radiative cooling using near-black infrared emitters. ACS Photon. 2017;4(3):626-630.
- 37. Zhang X, Qiu J, Zhao J, Li X, Liu L. Complex refractive indices measurements of polymers in infrared bands. *J Quant Spectrosc Radiat Transf.* 2020;252:107063.
- 38. Zhang X, Qiu J, Li X, Zhao J, Liu L. Complex refractive indices measurements of polymers in visible and near-infrared bands. *Appl Opt.* 2020;59(8):2337-2344.
- Palik ED. Handbook of Optical Constants of Solids. Vol 3. Academic Press; 1998.
- Bohren CF, Huffman DR. Absorption and Scattering of Light by Small Particles. John Wiley & Sons; 2008.
- 41. Modest MF. Radiative Heat Transfer. Academic press; 2013.
- 42. Granqvist C, Hjortsberg A. Radiative cooling to low temperatures: general considerations and application to selectively emitting SiO films. *J Appl Phys.* 1981;52(6):4205-4220.

How to cite this article: Fu Y, An Y, Xu Y, Dai J-G, Lei D. Polymer coating with gradient-dispersed dielectric nanoparticles for enhanced daytime radiative cooling. *EcoMat.* 2022;4(2): e12169. doi:10.1002/eom2.12169